Discontinuous Galerkin method for convection-dominated time-dependent PDEs

Chi-Wang Shu

Division of Applied Mathematics

Brown University

Outline

- Hyperbolic equations
- Convection-diffusion equations
- Higher order PDEs

Hyperbolic equations

Setup of the Runge-Kutta DG schemes

We are interested in solving a hyperbolic conservation law

$$u_t + f(u)_x = 0$$

In 2D it is

$$u_t + f(u)_x + g(u)_y = 0$$

and in system cases u is a vector, and the Jacobian $f'(u)$ is diagonalizable with real eigenvalues.

Several properties of the solutions to hyperbolic conservation laws.

- The solution u may become discontinuous regardless of the smoothness of the initial conditions.
- Weak solutions are not unique. The unique, physically relevant entropy solution satisfies additional entropy inequalities

$$U(u)_t + F(u)_x \leq 0$$

in the distribution sense, where $U(u)$ is a convex scalar function of u and the entropy flux $F(u)$ satisfies $F'(u) = U'(u)f'(u)$.

To solve the hyperbolic conservation law:

$$u_t + f(u)_x = 0, \tag{1}$$

we multiply the equation with a test function v, integrate over a cell $I_j = [x_{j-\frac{1}{2}}, x_{j+\frac{1}{2}}]$, and integrate by parts:

$$\int_{I_j} u_t v dx - \int_{I_j} f(u) v_x dx + f(u_{j+\frac{1}{2}}) v_{j+\frac{1}{2}} - f(u_{j-\frac{1}{2}}) v_{j-\frac{1}{2}} = 0$$

Now assume both the solution u and the test function v come from a finite dimensional approximation space V_h, which is usually taken as the space of piecewise polynomials of degree up to k:

$$V_h = \left\{ v : v|_{I_j} \in P^k(I_j), \; j = 1, \cdots, N \right\}$$

However, the boundary terms $f(u_{j+\frac{1}{2}})$, $v_{j+\frac{1}{2}}$ etc. are not well defined when u and v are in this space, as they are discontinuous at the cell interfaces.

From the conservation and stability (upwinding) considerations, we take

- A single valued monotone numerical flux to replace $f(u_{j+\frac{1}{2}})$:

$$\hat{f}_{j+\frac{1}{2}} = \hat{f}(u^-_{j+\frac{1}{2}}, u^+_{j+\frac{1}{2}})$$

  where $\hat{f}(u,u) = f(u)$ (consistency); $\hat{f}(\uparrow, \downarrow)$ (monotonicity) and $\hat{f}$ is Lipschitz continuous with respect to both arguments.

- Values from inside I_j for the test function v

$$v^-_{j+\frac{1}{2}}, \qquad v^+_{j-\frac{1}{2}}$$

Hence the DG scheme is: find $u \in V_h$ such that

$$\int_{I_j} u_t v dx - \int_{I_j} f(u) v_x dx + \hat{f}_{j+\frac{1}{2}} v^-_{j+\frac{1}{2}} - \hat{f}_{j-\frac{1}{2}} v^+_{j-\frac{1}{2}} = 0 \qquad (2)$$

for all $v \in V_h$.

Notice that, for the piecewise constant $k = 0$ case, we recover the well known first order monotone finite volume scheme:

$$(u_j)_t + \frac{1}{h}\left(\hat{f}(u_j, u_{j+1}) - \hat{f}(u_{j-1}, u_j)\right) = 0.$$

Time discretization could be by the TVD Runge-Kutta method (Shu and Osher, JCP 88). For the semi-discrete scheme:

$$\frac{du}{dt} = L(u)$$

where $L(u)$ is a discretization of the spatial operator, the third order TVD Runge-Kutta is simply:

$$\begin{aligned} u^{(1)} &= u^n + \Delta t L(u^n) \\ u^{(2)} &= \frac{3}{4}u^n + \frac{1}{4}u^{(1)} + \frac{1}{4}\Delta t L(u^{(1)}) \\ u^{n+1} &= \frac{1}{3}u^n + \frac{2}{3}u^{(2)} + \frac{2}{3}\Delta t L(u^{(2)}) \end{aligned}$$

Properties of DG schemes

The DG scheme has the following properties:

- Easy handling of complicated geometry and boundary conditions (common to all finite element methods). Allowing hanging nodes in the mesh (more convenient for DG);
- Compact. Communication only with immediate neighbors, regardless of the order of the scheme;

- Explicit. Because of the discontinuous basis, the mass matrix is local to the cell, resulting in explicit time stepping (no systems to solve);
- Parallel efficiency. Achieves 99% parallel efficiency for static mesh and over 80% parallel efficiency for dynamic load balancing with adaptive meshes (Biswas, Devine and Flaherty, APNUM 94; Remacle, Flaherty and Shephard, SIAM Rev 03); Also friendly to GPU environment (Klockner, Warburton, Bridge and Hesthaven, JCP10).

- Provable cell entropy inequality and L^2 stability, for arbitrary nonlinear equations in any spatial dimension and any triangulation, for any polynomial degrees, without limiters or assumption on solution regularity (Jiang and Shu, Math. Comp. 94 (scalar case); Hou and Liu, JSC 07 (symmetric systems)). For $U(u) = \frac{u^2}{2}$:

$$\frac{d}{dt}\int_{I_j} U(u)dx + \hat{F}_{j+1/2} - \hat{F}_{j-1/2} \leq 0$$

Summing over j: $\frac{d}{dt}\int_a^b u^2 dx \leq 0.$

This also holds for fully discrete RKDG methods with third order TVD Runge-Kutta time discretization, for linear equations (Zhang and Shu, SINUM 10).

- At least $(k+\frac{1}{2})$-th order accurate, and often $(k+1)$-th order accurate for smooth solutions when piecewise polynomials of degree k are used, regardless of the structure of the meshes, for smooth solutions (Lesaint and Raviart 74; Johnson and Pitkäranta, Math. Comp. 86 (linear steady state); Meng, Shu and Wu, Math. Comp. submitted (upwind-biased fluxes); Zhang and Shu, SINUM 04 and 06 (RKDG for nonlinear equations)).
- $(2k+1)$-th order superconvergence in negative norm and in strong L^2-norm for post-processed solution for linear and nonlinear equations with smooth solutions (Cockburn, Luskin, Shu and Süli, Math. Comp. 03; Ryan, Shu and Atkins, SISC 05; Curtis, Kirby, Ryan and Shu, SISC 07; Ji, Xu and Ryan, JSC 13).

- $(k+3/2)$-th or $(k+2)$-th order superconvergence of the DG solution to a special projection of the exact solution, and non-growth of the error in time up to $t = O(\frac{1}{\sqrt{h}})$ or $t = O(\frac{1}{h})$, for linear and nonlinear hyperbolic and convection diffusion equations (Cheng and Shu, JCP 08; Computers & Structures 09; SINUM 10; Meng, Shu, Zhang and Wu, SINUM 12 (nonlinear); Yang and Shu, SINUM 12 ($(k+2)$-th order)).

- Several formulations of DG methods for solving nonlinear Hamilton-Jacobi equations

$$\varphi_t + H(\varphi_x, \varphi_y) = 0$$

  - Using the DG method for the system satisfied by $(u, v) = (\varphi_x, \varphi_y)$ (Hu and Shu, SISC 99; Li and Shu, Applied Mathematics Letters 05; Xiong, Shu and Zhang, IJNAM 13).
  - Directly solving for φ (Cheng and Shu, JCP 07; Bokanowski, Cheng and Shu, SISC 11; Num. Math. 14; Xiong, Shu and Zhang, IJNAM 13).
  - An LDG method (Yan and Osher, JCP 11; Xiong, Shu and Zhang, IJNAM 13).

- Easy h-p adaptivity.
- Stable and convergent DG methods are now available for many nonlinear PDEs containing higher derivatives: convection diffusion equations, KdV equations, ...

Systems and multi-dimensions, unstructured meshes

The RKDG method applies in the same form to hyperbolic systems. The only difference is that monotone numerical fluxes are replaced by numerical fluxes based on exact or approximate Riemann solvers (Godunov, Lax-Friedrichs, HLLC, etc. See Toro, Springer 99). Local characteristic decomposition is not needed unless a nonlinear limiter is used.

The RKDG method applies in the same way to multi-dimensional problems including unstructured meshes. Integration by parts is replaced by divergence theorem. Numerical fluxes are still one-dimensional in the normal direction of the cell boundary.

History and references

Here is a (very incomplete) history of the early study of DG methods for convection dominated problems:

- 1973: First discontinuous Galerkin method for steady state linear scalar conservation laws (Reed and Hill).
- 1974: First error estimate (for tensor product mesh) of the discontinuous Galerkin method of Reed and Hill (Lesaint and Raviart).
- 1986: Error estimates for discontinuous Galerkin method of Reed and Hill (Johnson and Pitkäranta).
- 1989-1998: Runge-Kutta discontinuous Galerkin method for *nonlinear* conservation laws (Cockburn, Shu, ...).

- 1994: Proof of cell entropy inequality for discontinuous Galerkin method for nonlinear conservation laws in general multidimensional triangulations (Jiang and Shu).
- 1997-1998: Discontinuous Galerkin method for convection diffusion problems (Bassi and Rebay, Cockburn and Shu, Baumann and Oden, ...).
- 2002: Discontinuous Galerkin method for partial differential equations with third or higher order spatial derivatives (KdV, biharmonic, ...) (Yan and Shu, Xu and Shu, ...)

Collected works on the DG methods:

- Discontinuous Galerkin Methods: Theory, Computation and Applications, B. Cockburn, G. Karniadakis and C.-W. Shu, editors, Lecture Notes in Computational Science and Engineering, volume 11, Springer, 2000. (Proceedings of the first DG Conference)
- Journal of Scientific Computing, special issue on DG methods, 2005.
- Computer Methods in Applied Mechanics and Engineering, special issue on DG methods, 2006.
- Journal of Scientific Computing, special issue on DG methods, 2009.

- Li, Discontinuous Finite Elements in Fluid Dynamics and Heat Transfer, Birkhauser 2006.
- Kanschat, Discontinuous Galerkin Methods for Viscous Flow, Deutscher Universitätsverlag, Wiesbaden 2007.
- Hesthaven and Warburton, Nodal Discontinuous Galerkin Methods, Springer 2008.
- Rivière, Discontinuous Galerkin Methods for Solving Elliptic and Parabolic Equations. Theory and Implementation, SIAM 2008.

- Shu, Discontinuous Galerkin methods: general approach and stability, in S. Bertoluzza, S. Falletta, G. Russo, and C.-W. Shu, editors, *Numerical Solutions of Partial Differential Equations*, pages 149–201. Birkhäuser 2009.
- Di Pietro and Ern, Mathematical Aspects of Discontinuous Galerkin Methods, Springer 2012.
- Marica and Zuazua, Symmetric Discontinuous Galerkin Methods for 1-D Waves, Springer 2014.

Three examples

We show three examples to demonstrate the excellent performance of the DG method.

The first example is the linear convection equation

$$u_t + u_x = 0, \qquad or \qquad u_t + u_x + u_y = 0,$$

on the domain $(0, 2\pi) \times (0, T)$ or $(0, 2\pi)^2 \times (0, T)$ with the characteristic function of the interval $(\frac{\pi}{2}, \frac{3\pi}{2})$ or the square $(\frac{\pi}{2}, \frac{3\pi}{2})^2$ as initial condition and periodic boundary conditions.

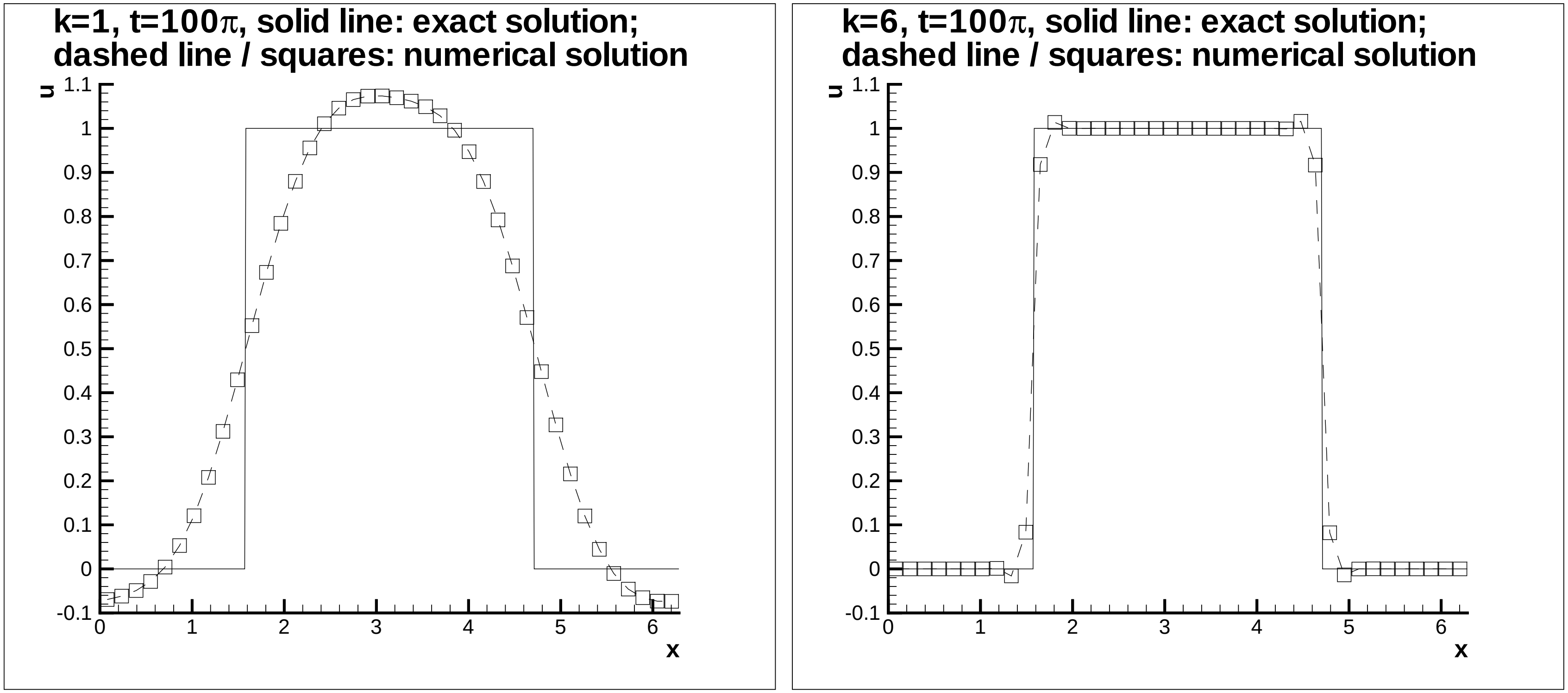

Figure 1: Transport equation: Comparison of the exact and the RKDG solutions at $T = 100\pi$ with second order (P^1, left) and seventh order (P^6, right) RKDG methods. One dimensional results with 40 cells, exact solution (solid line) and numerical solution (dashed line and symbols, one point per cell)

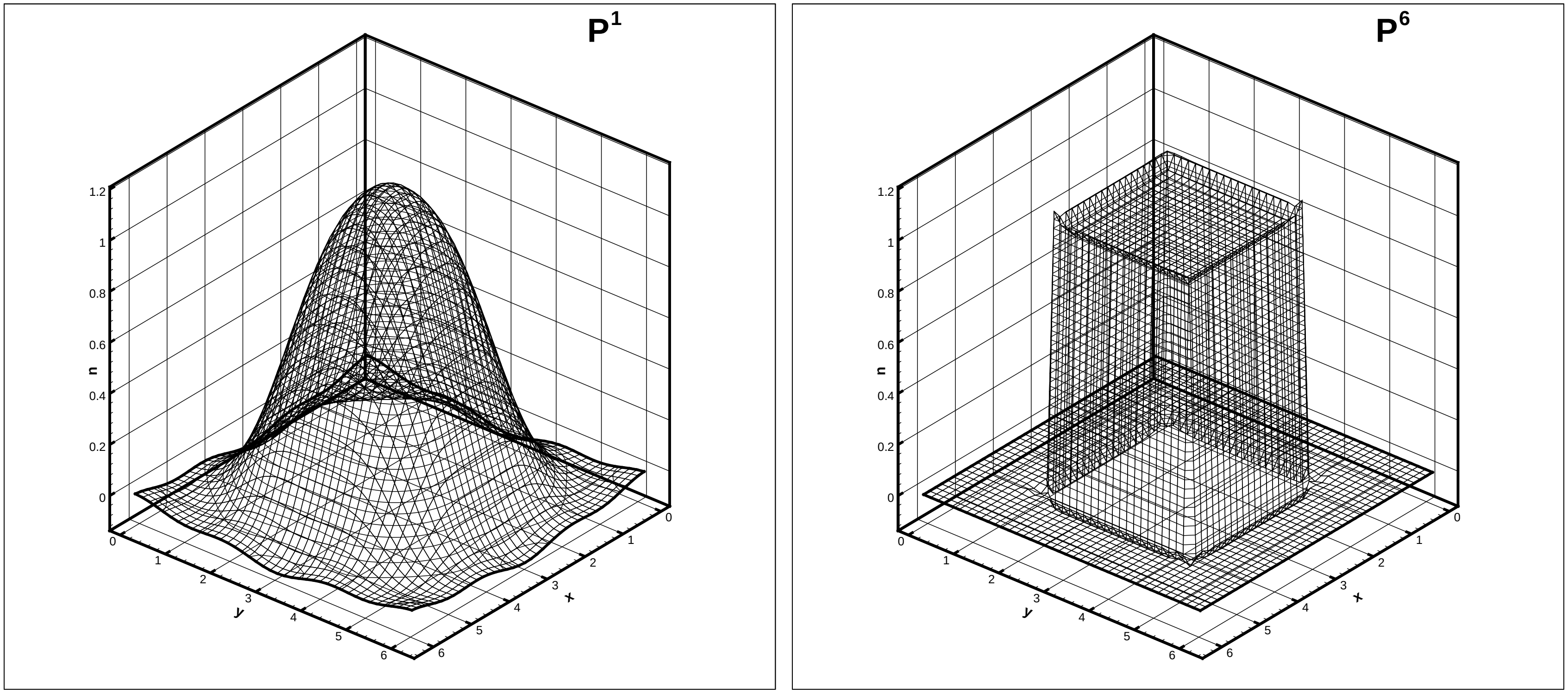

Figure 2: Transport equation: Comparison of the exact and the RKDG solutions at $T = 100\pi$ with second order (P^1, left) and seventh order (P^6, right) RKDG methods. Two dimensional results with 40×40 cells.

The second example is the double Mach reflection problem for the two dimensional compressible Euler equations.

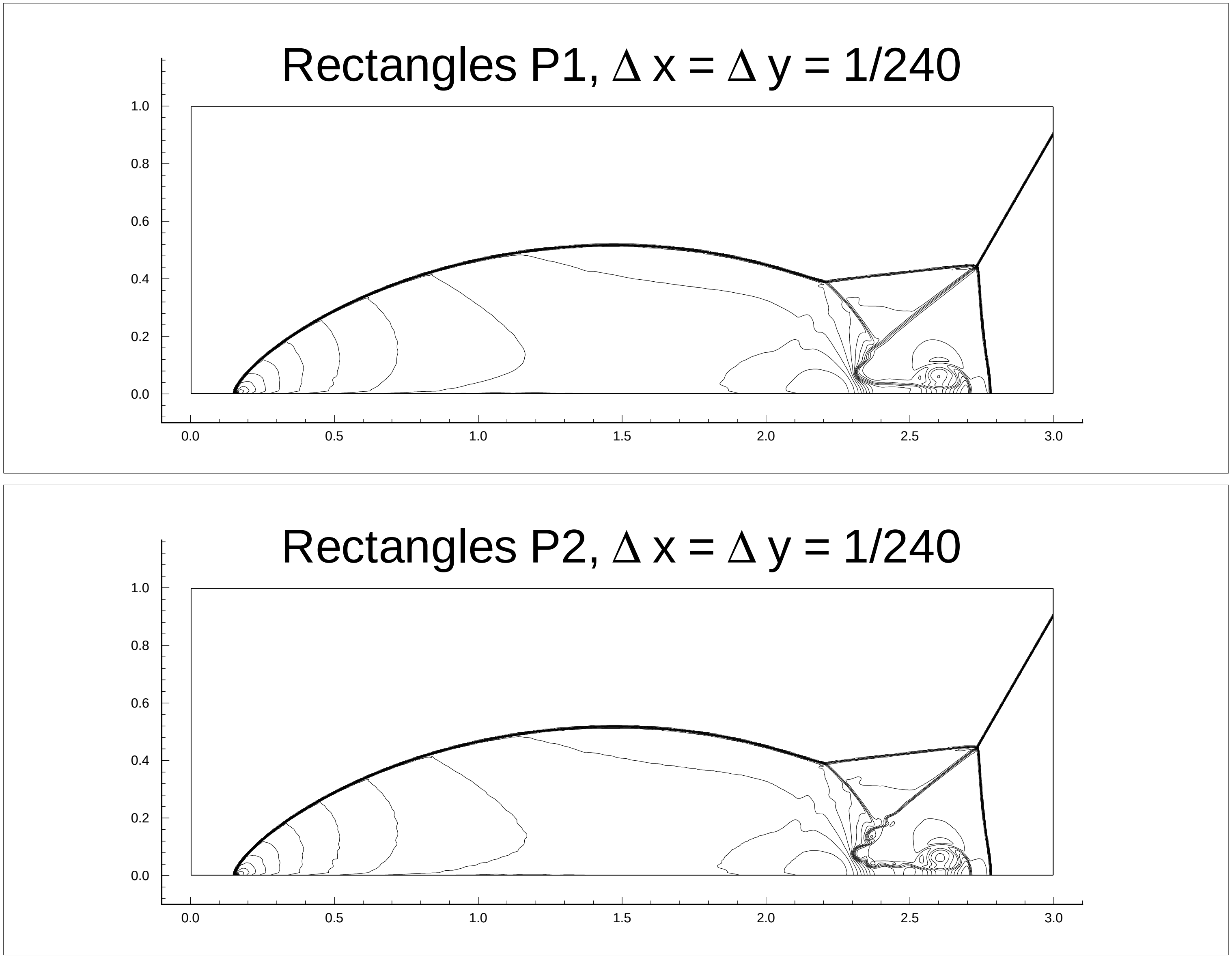

Figure 3: Double Mach reflection. $\Delta x = \Delta y = \frac{1}{240}$. Top: P^1; bottom: P^2.

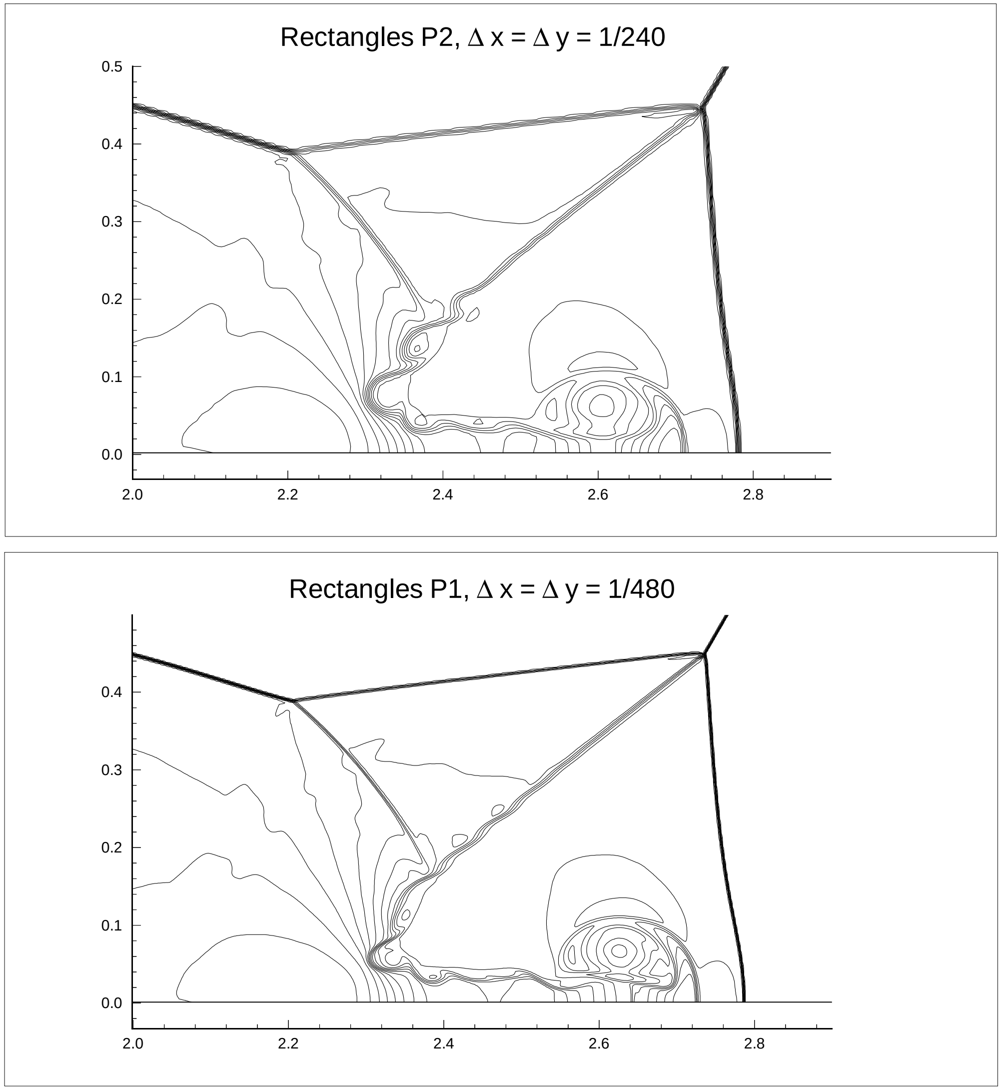

Figure 4: Double Mach reflection. Zoomed-in region. Top: P^2 with $\Delta x = \Delta y = \frac{1}{240}$; bottom: P^1 with $\Delta x = \Delta y = \frac{1}{480}$.

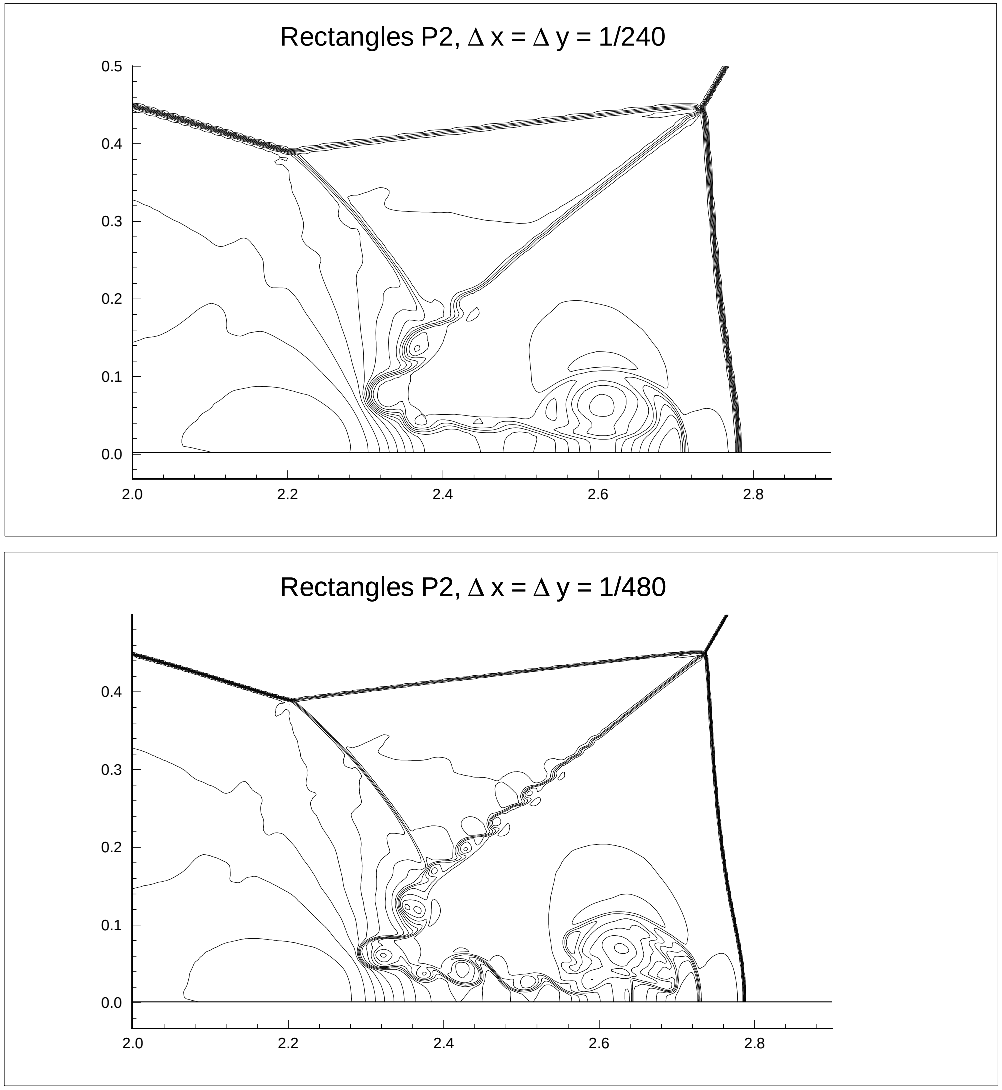

Figure 5: Double Mach reflection. Zoomed-in region. P^2 elements. Top: $\Delta x = \Delta y = \frac{1}{240}$; bottom: $\Delta x = \Delta y = \frac{1}{480}$.

The third example is the flow past a forward-facing step problem for the two dimensional compressible Euler equations. No special treatment is performed near the corner singularity.

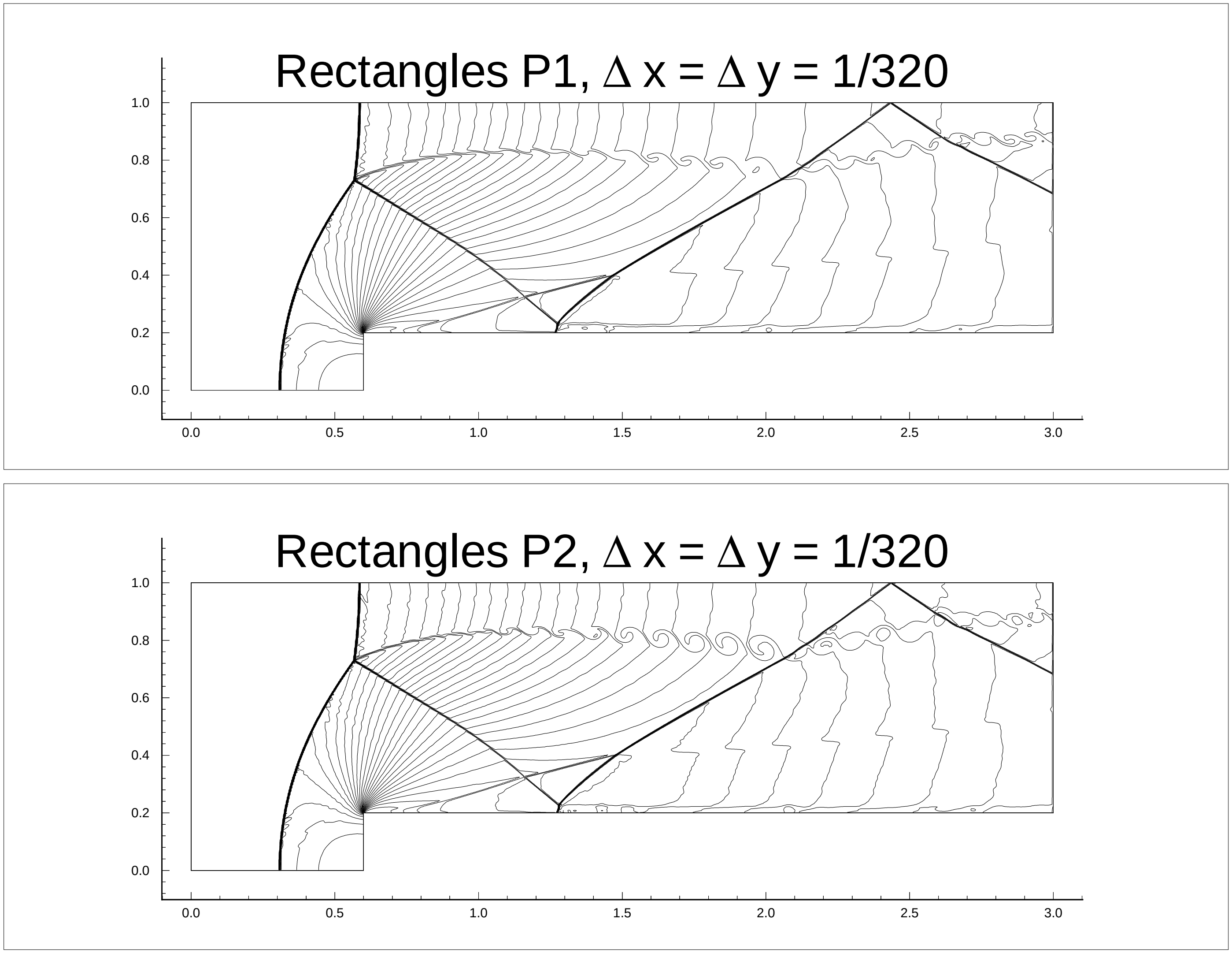

Figure 6: Forward facing step. Zoomed-in region. $\Delta x = \Delta y = \frac{1}{320}$. Left: P^1 elements; right: P^2 elements.

Relationship with CPR schemes

The correction procedure via reconstruction (CPR), by Huynh, AIAA papers 2007-4079, 2009-403; Wang and Gao, JCP 09; and Haga, Gao and Wang, Math. Model. Nat. Phenom. 11, is an extension of the spectral finite volume and spectral finite difference methods and can be summarized as follows.

We solve

$$u_t + f(u)_x = 0$$

with the same notation as in DG. $I_j = [x_{j-1/2}, x_{j+1/2}]$ contains $k+1$ "solution points"

$$x_{j-1/2} \leq x_{j,0} < x_{j,1} < \ldots < x_{j,k} \leq x_{j+1/2}.$$

The computational degrees of freedom are $u_{j,i}$, which approximate the exact solution at the solution points $u(x_{j,i}, t)$ for $i = 0, 1, \ldots, k$ and all cells I_j.

- Given $u_{j,i}$, obtain an interpolation polynomial $u_j(x)$ of degree at most k which satisfies $u_j(x_{j,i}) = u_{j,i}$.
- Obtain the "discontinuous flux function" $f_j(x)$, which is an interpolation polynomial of degree at most k which satisfies $f_j(x_{j,i}) = f(u_{j,i})$.
- Compute the left and right limits of the discontinuous interpolation polynomials at $x_{j+1/2}$, namely $u^-_{j+1/2} = u_j(x_{j+1/2})$ and $u^+_{j+1/2} = u_{j+1}(x_{j+1/2})$, then form a numerical flux using any monotone flux (approximate Riemann solver) $\hat{f}_{j+1/2} = \hat{f}(u^-_{j+1/2}, u^+_{j+1/2})$.

- Form a “continuous flux function” $F_j(x)$, which is a polynomial of degree at most $k+1$, satisfying $F_j(x_{j-1/2}) = \hat{f}_{j-1/2}$ and $F_j(x_{j+1/2}) = \hat{f}_{j+1/2}$, and is a good approximation of the discontinuous flux function $f_j(x)$ inside cell I_j.

One way to form $F_j(x)$ is by

$$\begin{aligned} F_j(x) &= f_j(x) + (\hat{f}_{j-1/2} - f_j(x_{j-1/2}))g_\ell(x) \\ &\quad + (\hat{f}_{j+1/2} - f_j(x_{j+1/2}))g_r(x) \end{aligned}$$

where the left correction function $g_\ell(x)$ is a polynomial of degree at most $k+1$ which satisfies

$$g_\ell(x_{j-1/2}) = 1, \qquad g_\ell(x_{j+1/2}) = 0,$$

and likewise the right correction function $g_r(x)$ is a polynomial of degree at most $k+1$ which satisfies

$$g_r(x_{j-1/2}) = 0, \qquad g_r(x_{j+1/2}) = 1.$$

- The evolution of the computational degrees of freedom is thus simply

$$\frac{d}{dt}u_{j,i} = -(F_j)_x(x_{j,i}), \qquad i = 0, ..., k, \ \forall j$$

Notice that there are still $k-1$ degrees of freedom in the design of each of the left and right correction functions $g_\ell(x)$ and $g_r(x)$. It can be shown that a particular choice of $g_\ell(x)$ and $g_r(x)$ will lead to the fact that the CPR scheme thus constructed is exactly equivalent to the DG scheme for the linear case $f(u) = au$. Therefore, even for the nonlinear case, the CPR scheme can be considered as equivalent to the DG scheme with a suitable numerical quadrature.

Selected issues of current interest

Limiters

The RKDG schemes for conservation laws are energy stable (L^2 stable). However, for solving problems with strong discontinuities, the DG solution may generate spurious numerical oscillations. In practice, especially for nonlinear problems containing strong shocks, we often need to apply nonlinear limiters to control these oscillations. Most of the limiters studied in the literature come from the methodologies of finite volume high resolution schemes.

A limiter can be considered as a post-processor of the computed DG solution. In any cell which is deemed to contain a possible discontinuity (the so-called troubled cells), the DG polynomial is replaced by a new polynomial of the same degree, while maintaining the original cell average for conservation.

Some commonly used limiters:

- The total variation diminishing (TVD) limiters (Harten, JCP 83).
  - The new polynomial is less oscillatory than the old one.
  - If the solution in this cell happens to be smooth but is near an extrema, then the new polynomial may degenerate to first order accuracy.
  - The limiter is reasonably easy to implement on structured meshes but more difficult to implement on unstructured meshes. It does not involve any user-tuned parameters.
  - The limited scheme is TVDM (total variation diminishing in the means)

- The total variation bounded (TVB) limiters (Shu, Math Comp 87).
  - The new polynomial is less oscillatory than the old one.
  - If the solution in this cell happens to be smooth, then the limiter does not take effect and hence the new polynomial is the same as the old polynomial with of course the same high order accuracy.
  - The limiter is reasonably easy to implement on structured meshes but more difficult to implement on unstructured meshes. It does involve a user-tuned parameter M which is related to the second derivative of the solution at smooth extrema.
  - The limited scheme is TVB (total variation bounded).

- The moment-based limiters (Biswas et al. Appl. Num. Math. 94; Burbeau et al. JCP 01)
  - The new polynomial is less oscillatory than the old one.
  - If the solution in this cell happens to be smooth, the limiter could still degenerate the accuracy to first order.
  - The limiter is reasonably easy to implement on structured meshes but more difficult to implement on unstructured meshes. It does not involve any user-tuned parameters.
  - The limited scheme cannot be proved to be total variation stable.

- WENO (weighted essentially non-oscillatory) limiters (Qiu and Shu, JCP 03; SISC 05; Computers & Fluids 05; Zhu, Qiu, Shu and Dumbser, JCP 08; Zhu and Qiu, JCP 12. Zhong and Shu, JCP 13; Zhu, Zhong, Shu and Qiu, JCP 13). They have also been extended to CPR schemes (Du, Shu and Zhang, Appl. Num. Math., to appear).
  - The new polynomial is less oscillatory than the old one.
  - If the solution in this cell happens to be smooth, the limiter will maintain the original high order of accuracy.
  - The most recent WENO limiter of Zhong et al. is very easy to implement, especially on unstructured meshes. It does not involve any user-tuned parameters.
  - The limited scheme cannot be proved to be total variation stable.

Bound-preserving high order accuracy limiter

For the scalar conservation laws

$$u_t + \nabla \cdot \mathbf{F}(u) = 0, \qquad u(\mathbf{x}, 0) = u_0(\mathbf{x}), \tag{3}$$

An important property of the entropy solution (which may be discontinuous) is that it satisfies a strict maximum principle: If

$$M = \max_{\mathbf{x}} u_0(\mathbf{x}), \quad m = \min_{\mathbf{x}} u_0(\mathbf{x}), \tag{4}$$

then $u(\mathbf{x}, t) \in [m, M]$ for any $\mathbf{x}$ and t.

For nonlinear systems, the bound to maintain would be physically relevant, for example the positivity of density and pressure for compressible gas dynamics, the positivity of water height for shallow water equations, the positivity of probability density functions, etc.

It is a challenge to design simple limiters which can maintain these bounds numerically while still keeping the original high order accuracy of the DG scheme. I will provide more details on recent developments in this area in my talk later in this conference.

Error estimates for discontinuous solutions

While there are many results on convergence and error estimates for DG methods with smooth solutions, the study for discontinuous solutions is more challenging.

- Johnson et al CMAME 84; Johnson and Pitkäranta Math Comp 86; Johnson et al Math Comp 87: error estimates for piecewise linear streamline diffusion and DG methods for stationary (or space-time) linear hyperbolic equations. Pollution region around discontinuity: $\mathcal{O}(h^{1/2}\log(1/h))$.

- Cockburn and Guzmán SINUM 08: RKDG2 (second order in space and time) for linear hyperbolic equations. Pollution region around discontinuity: $\mathcal{O}(h^{1/2}\log(1/h))$ on the downwind side and $\mathcal{O}(h^{2/3}\log(1/h))$ on the upwind side.
- Zhang and Shu, Num Math 14: RKDG3 scheme with arbitrary polynomial degree $k \geq 1$ in space and third order TVD Runge-Kutta in time, on arbitrary quasi-uniform mesh.

Theorem: Assume the CFL number $\lambda := |\beta|\Delta t/h_{\min}$ is small enough, there holds

$$\|u(t^N) - u_h^N\|_{L^2(\mathbb{R}\backslash\mathcal{R}_T)} \leq M(h^{k+1} + \Delta t^3), \tag{5}$$

where $M > 0$ is independent of h and Δt, but may depend on the final time T, the norm of the exact solution in smooth regions, and the jump at the discontinuity point. Here $\mathcal{R}_T$ is the pollution region at the final time T, given by

$$\mathcal{R}_T = (\beta T - C\sqrt{T\beta\nu^{-1}}h^{1/2}\log(1/h), \beta T + C\sqrt{T\beta\nu^{-1}}h^{1/2}\log(1/h)) \tag{6}$$

where $C > 0$ is independent of $\nu = h_{\min}/h_{\max}, \lambda, \beta, h, \Delta t$ and T.

Note: Pollution region around discontinuity: $\mathcal{O}(h^{1/2}\log(1/h))$ on both sides of the discontinuity. This is numerically verified to be sharp for at least $k = 2$ and $k = 3$ (spatially third and fourth order accuracy).

DG method for front propagation with obstacles

We consider the following equation

$$\min(u_t + H(x, \nabla u),\ u - g(x)) = 0, \quad x \in R^d, \quad t > 0, \tag{7}$$

together with an initial condition. Here $g(x)$ is the “obstacle function”, and (7) is referred as the “obstacle equation”.

It was remarked in (Bokanowski, Forcadel and Zidani, SIAM J. Control Opt. 10) that (7) could be used to code the reachable sets of optimal control problems by using u as a level set function. It can be used to recover various objects such as the minimal time function.

In (Bokanowski, Cheng and Shu, Num Math 14), we propose fully discrete and explicit RKDG methods for (7).

Compared to traditional finite element methods for such problems, the DG scheme proposed does not require solving a nonlinear equation at each time step. Rather, the obstacles are incorporated by a simple projection step given explicitly through a comparison with the obstacle functions at Gaussian quadrature points.

We derive stability estimates for these fully discrete schemes, in the particular case where $H(x, \nabla u)$ is linear in ∇u (although the equation is nonlinear because of the obstacle term). Convergence with error estimates is proved in (Bokanowski, Cheng and Shu, Math Comp submitted).

Example 1.

We consider

$$f(t,x,y) := sign\left(\frac{T}{2}-t\right)\begin{pmatrix} -2\pi\ y \\ 2\pi\ x \end{pmatrix}\max(1-\|\mathbf{x}\|_2,0).$$

where $\|\mathbf{x}\|_2 := \sqrt{x^2+y^2}$ and with a Lipschitz continuous initial data φ:

$$\varphi^0(x,y) = \min(\max(y,-1),1). \tag{8}$$

The function φ^0 has a 0-level set which is the x axis. In this example the front evolves up to time $t = T/2$ then it comes back to the initial data at time $t = T$. $T/2$ represents the number of turns.

Computations have been done up to time $T = 10$.

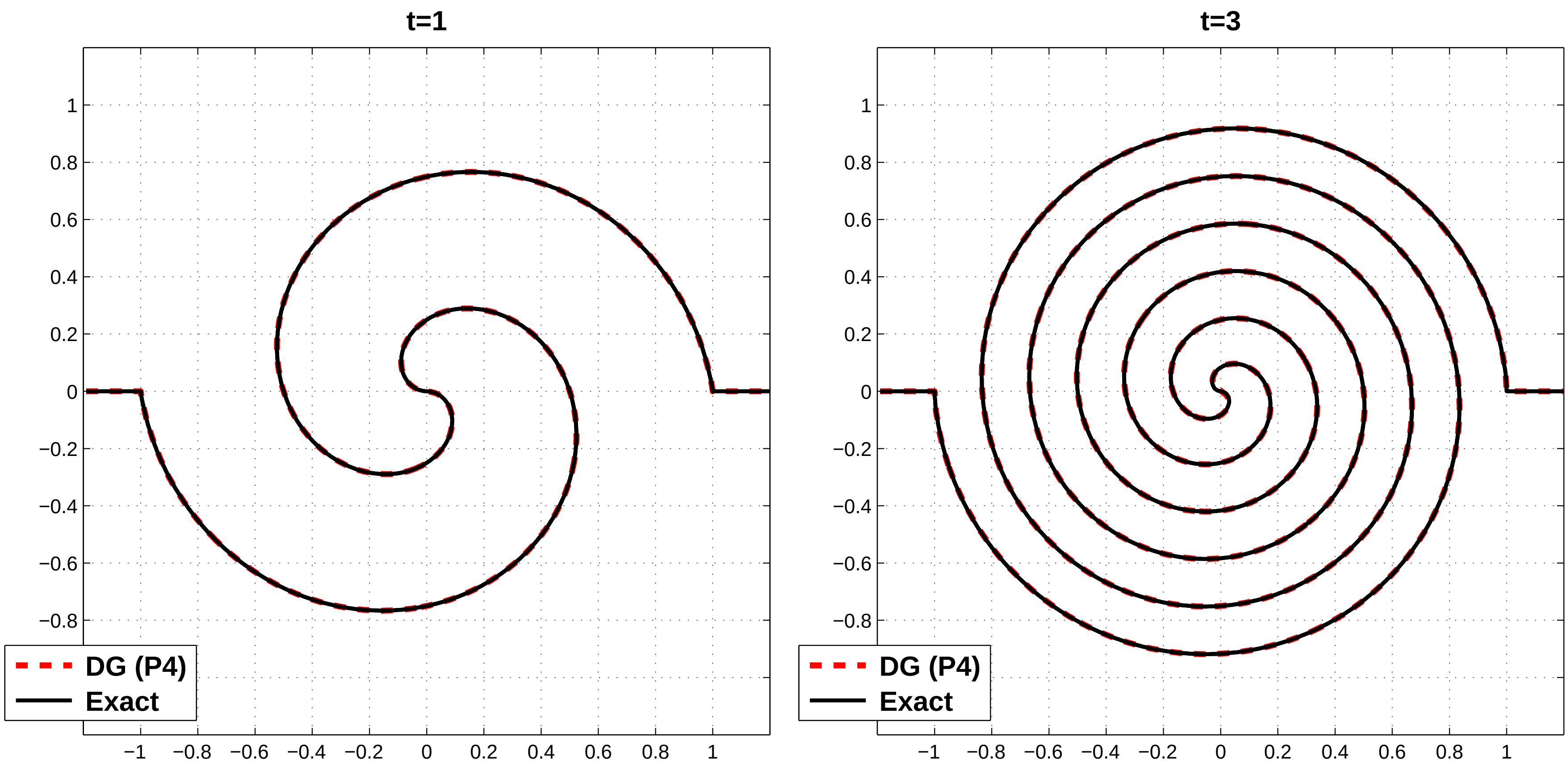

Figure 7: Example 1. Plots at times $t = 1$ and $t = 3$ with P^4 and 24×24 mesh cells.

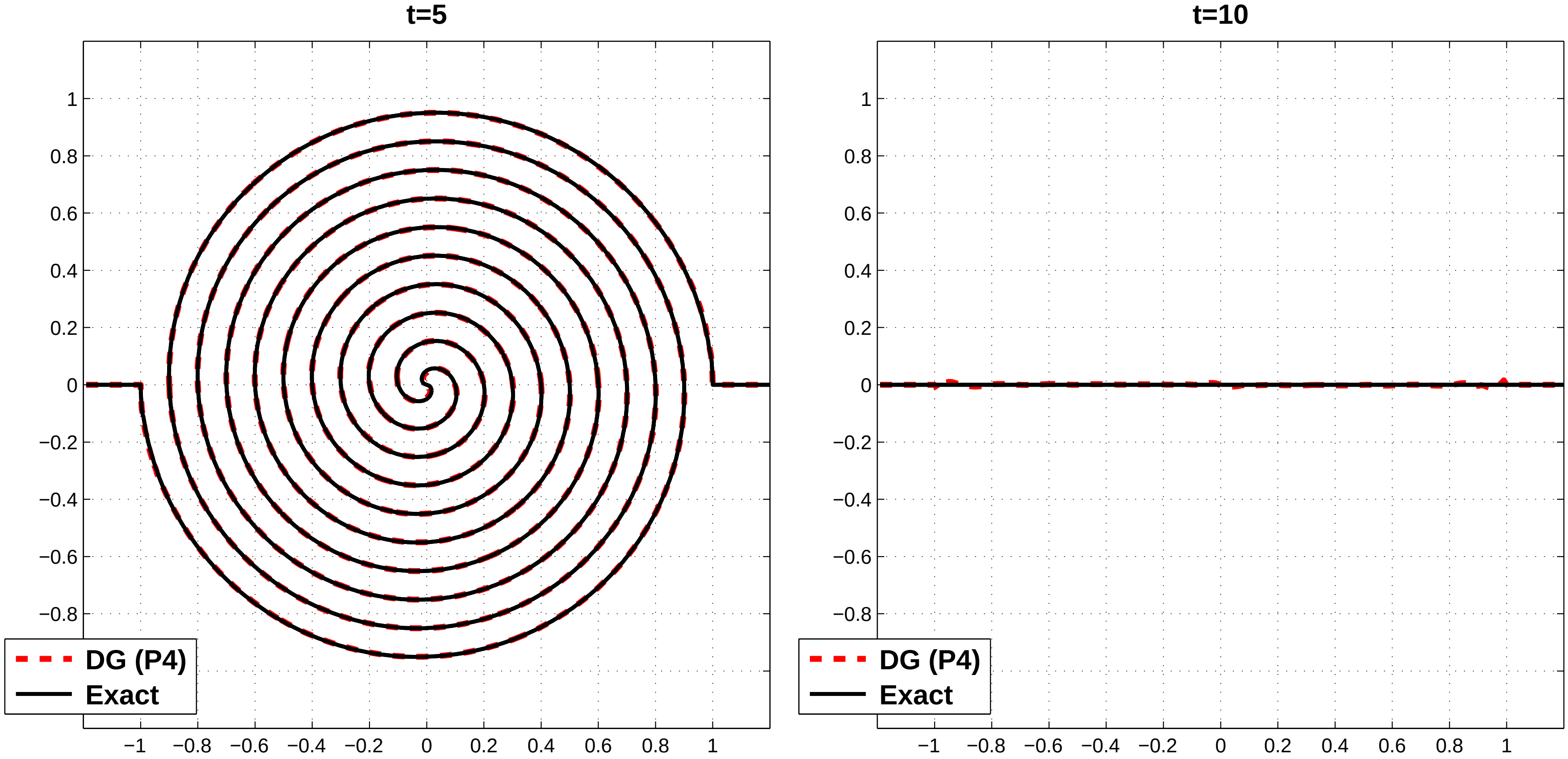

Figure 8: Example 1. Plots at times $t = 5$ and $t = 10$ (return to initial data), with P^4 and 24×24 mesh cells.

Example 2.

In this example we consider an initial data $u_0(x,y) := \|(x,y)-(1,0)\|_\infty - 0.5$, an obstacle coded by $g(x,y) := 0.5 - \|(x,y)-(0,\ 0.5)\|_\infty$, and the problem

$$\min(u_t + \max\left(0, 2\pi(-y,x)\cdot\nabla u\right), u - g(x,y)) = 0, \quad t>0,\ (x,y)$$

$$u(0,x,y) = u_0(x,y), \quad (x,y)\in\Omega,$$

The domain is $\Omega := [-2,2]^2$. Thus we want to compute the backward reachable set associated to the dynamics $f(x,y) = -2\pi(-y,x)$ and the target $T = \{(x,y), u_0(x,y)\le 0\}$, together with an obstacle or forbidden zone represented by $\{(x,y), g(x,y)\ge 0\}$.

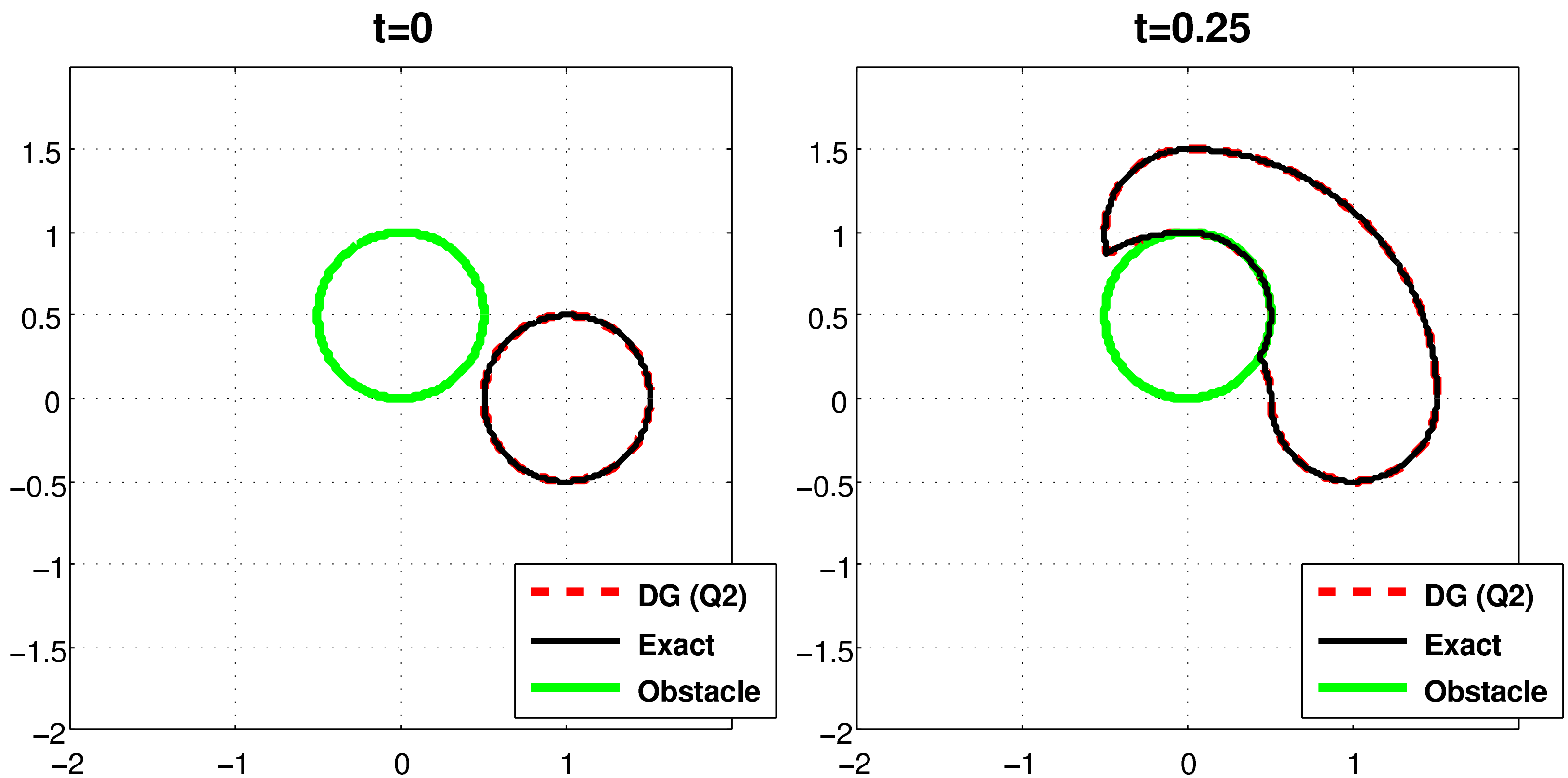

Figure 9: Example 2. Plots at times $t \in \{0,\ 0.25,\ 0.5,\ 0.75\}$, with Q^2 and 80×80 mesh cells.

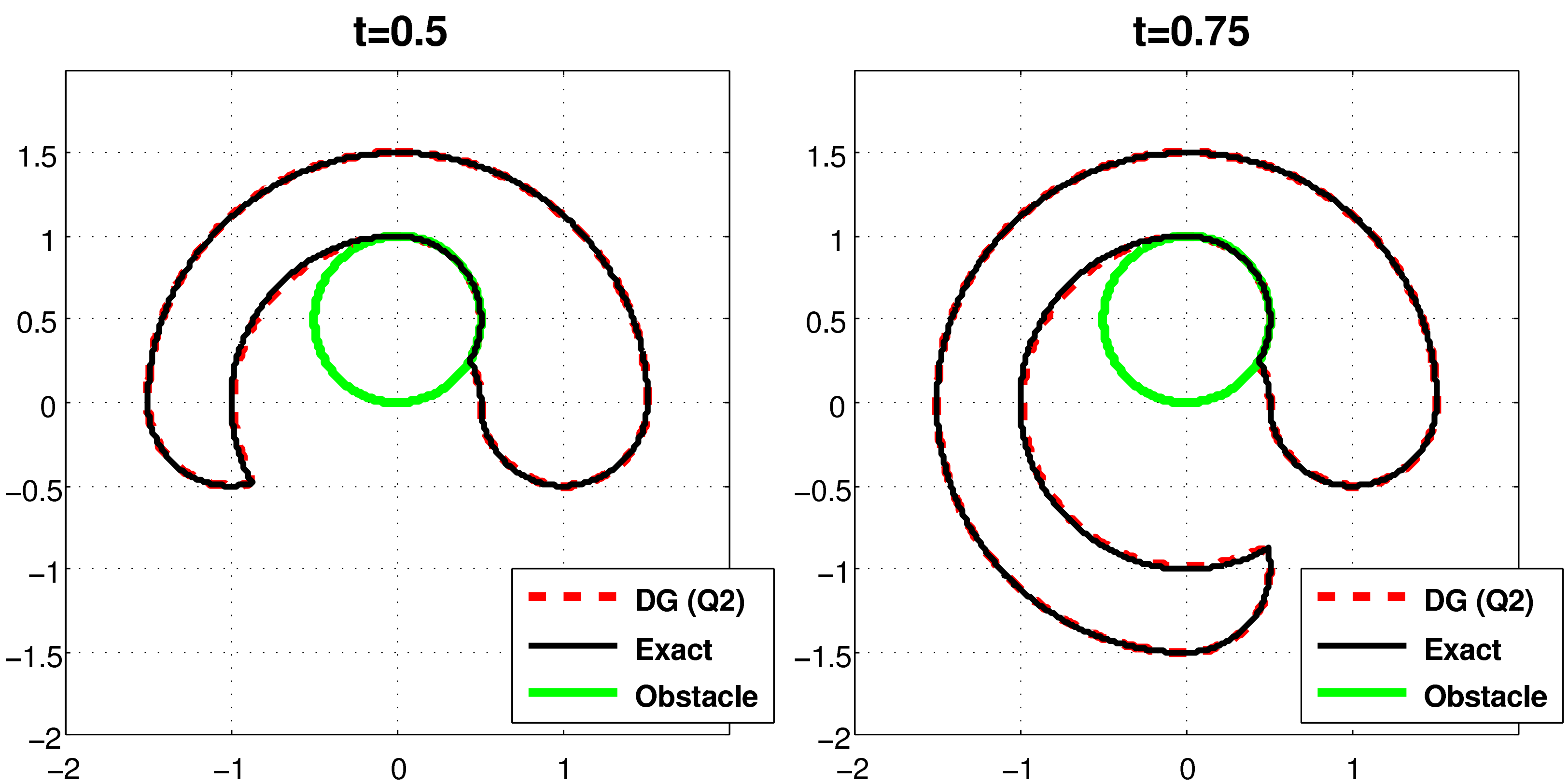

Figure 10: Example 2 (continued)

Convection-diffusion equations

A bad scheme

A naive generalization of the DG method to a PDE containing higher order spatial derivatives could have disastrous results.

Consider, as a simple example, the heat equation

$$u_t - u_{xx} = 0 \tag{9}$$

for $x \in [0, 2\pi]$ with periodic boundary conditions and with an initial condition $u(x, 0) = \sin(x)$.

A straightforward generalization of the DG method from the hyperbolic equation $u_t + f(u)_x = 0$ is to write down the same scheme and replace $f(u)$ by $-u_x$ everywhere: find $u \in V_h$ such that, for all test functions $v \in V_h$,

$$\int_{I_j} u_t v dx + \int_{I_j} u_x v_x dx - \hat{u_x}_{j+\frac{1}{2}} v^-_{j+\frac{1}{2}} + \hat{u_x}_{j-\frac{1}{2}} v^+_{j-\frac{1}{2}} = 0 \qquad (10)$$

Lacking an upwinding consideration for the choice of the flux $\hat{u_x}$ and considering that diffusion is isotropic, a natural choice for the flux could be the central flux

$$\hat{u_x}_{j+\frac{1}{2}} = \frac{1}{2}\left((u_x)^-_{j+\frac{1}{2}} + (u_x)^+_{j+\frac{1}{2}}\right)$$

However the result is horrible!

Table 1: L^2 and L^∞ errors and orders of accuracy for the "inconsistent" discontinuous Galerkin method (10) applied to the heat equation (9) with an initial condition $u(x, 0) = \sin(x)$, $t = 0.8$. Third order Runge-Kutta in time.

	$k=1$				$k=2$			
Δx	L^2 error	order	L^∞ error	order	L^2 error	order	L^∞ error	order
$2\pi/20$	1.78E-01	—	2.58E-01	—	1.85E-01	—	2.72E-01	—
$2\pi/40$	1.76E-01	0.016	2.50E-01	0.025	1.78E-01	0.049	2.55E-01	0.089
$2\pi/80$	1.75E-01	0.004	2.48E-01	0.012	1.77E-01	0.013	2.51E-01	0.025
$2\pi/160$	1.75E-01	0.001	2.48E-01	0.003	1.76E-01	0.003	2.50E-01	0.007

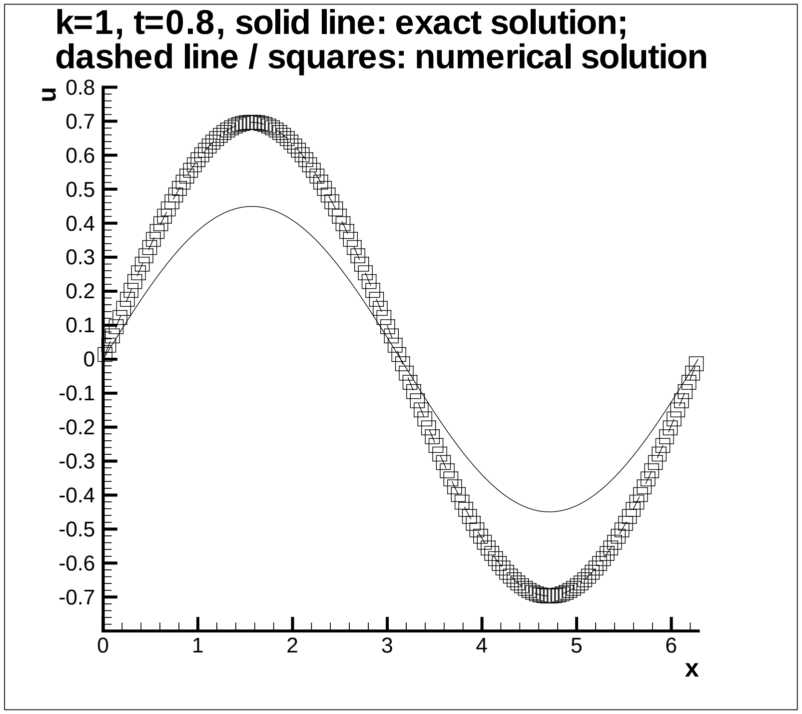

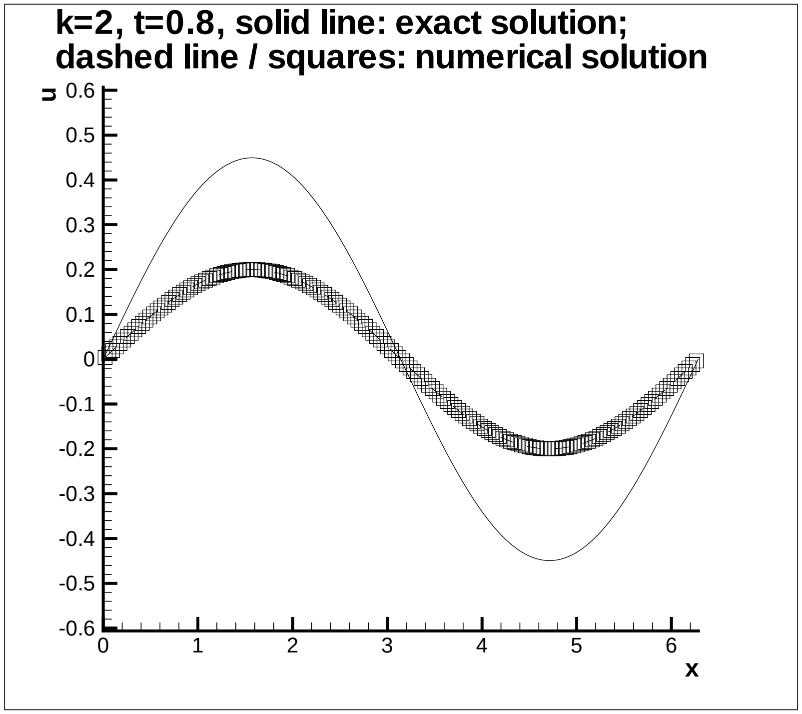

Figure 11: The “inconsistent” discontinuous Galerkin method (10) applied to the heat equation (9) with an initial condition $u(x,0) = \sin(x)$. $t = 0.8$. 160 cells. Third order Runge-Kutta in time. Solid line: the exact solution; Dashed line and squares symbols: the computed solution at the cell centers. Left: $k = 1$; Right: $k = 2$.

It is proven in Zhang and Shu, M^3AS 03, that this "inconsistent" DG method for the heat equation is actually

- consistent with the heat equation,
- but (very weakly) unstable.

LDG method for convection diffusion equations

A good DG method for the heat equation: the local DG (LDG) method (Bassi and Rebay, JCP 97; Cockburn and Shu, SINUM 98): rewrite the heat equation as

$$u_t - q_x = 0, \qquad q - u_x = 0, \tag{11}$$

and *formally* write out the DG scheme as: find $u, q \in V_h$ such that, for all test functions $v, w \in V_h$,

$$\begin{aligned} \int_{I_j} u_t v dx + \int_{I_j} q v_x dx - \hat{q}_{j+\frac{1}{2}} v^-_{j+\frac{1}{2}} + \hat{q}_{j-\frac{1}{2}} v^+_{j-\frac{1}{2}} &= 0 \\ \int_{I_j} q w dx + \int_{I_j} u w_x dx - \hat{u}_{j+\frac{1}{2}} w^-_{j+\frac{1}{2}} + \hat{u}_{j-\frac{1}{2}} w^+_{j-\frac{1}{2}} &= 0, \end{aligned} \tag{12}$$

q can be locally (within cell I_j) solved and eliminated, hence local DG.

A key ingredient of the design of the LDG method is the choice of the numerical fluxes $\hat{u}$ and $\hat{q}$ (remember: no upwinding principle for guidance).

The best choice for the numerical fluxes is the following alternating flux

$$\hat{u}_{j+\frac{1}{2}} = u^-_{j+\frac{1}{2}}, \qquad \hat{q}_{j+\frac{1}{2}} = q^+_{j+\frac{1}{2}}. \tag{13}$$

The other way around also works

$$\hat{u}_{j+\frac{1}{2}} = u^+_{j+\frac{1}{2}}, \qquad \hat{q}_{j+\frac{1}{2}} = q^-_{j+\frac{1}{2}}.$$

We then have

- L^2 stability
- optimal convergence of $O(h^{k+1})$ in L^2 for P^k elements

Table 2: L^2 and L^∞ errors and orders of accuracy for the LDG applied to the heat equation.

	$k=1$				$k=2$			
Δx	L^2 error	order	L^∞ error	order	L^2 error	order	L^∞ error	orde
$2\pi/20$, u	1.92E-03	—	7.34E-03	—	4.87E-05	—	2.30E-04	—
$2\pi/20$, q	1.93E-03	—	7.33E-03	—	4.87E-05	—	2.30E-04	—
$2\pi/40$, u	4.81E-04	2.00	1.84E-03	1.99	6.08E-06	3.00	2.90E-05	2.9
$2\pi/40$, q	4.81E-04	2.00	1.84E-03	1.99	6.08E-06	3.00	2.90E-05	2.9
$2\pi/80$, u	1.20E-04	2.00	4.62E-04	2.00	7.60E-07	3.00	3.63E-06	3.0
$2\pi/80$, q	1.20E-04	2.00	4.62E-04	2.00	7.60E-07	3.00	3.63E-06	3.0
$2\pi/160$, u	3.00E-05	2.00	1.15E-04	2.00	9.50E-08	3.00	4.53E-07	3.0
$2\pi/160$, q	3.00E-05	2.00	1.15E-04	2.00	9.50E-08	3.00	4.53E-07	3.0

The conclusions are valid for general nonlinear multi-dimensional convection diffusion equations

$$u_t + \sum_{i=1}^{d} f_i(u)_{x_i} - \sum_{i=1}^{d}\sum_{j=1}^{d}(a_{ij}(u)u_{x_j})_{x_i} = 0, \qquad (14)$$

where $a_{ij}(u)$ are entries of a symmetric and semi-positive definite matrix, Cockburn and Shu, SINUM 98; Xu and Shu, CMAME 07; Shu, Birkhäuser 09.

Other types of DG methods for diffusion equations

- Internal penalty DG methods: symmetric internal penalty discontinuous Galerkin (SIPG) method (Wheeler, SINUM 78; Arnold, SINUM 82); non-symmetric internal penalty discontinuous Galerkin (NIPG) method (Baumann and Oden, CMAME 99; Oden, Babuvska and Baumann, JCP 98)
- HDG method (attend the lectures by Professor Cockburn!)
- Direct discontinuous Galerkin (DDG) methods of Liu and Yan, SINUM 09, CiCP 10.
- Ultra weak discontinuous Galerkin methods (Cheng and Shu, Math Comp 08).

Selected issues of current interest

Multiscale DG method

We aim for obtaining small errors $||u - u_h||$ in a strong norm (typically L^2 norm) where the exact solution u has a small scale ε and the mesh size $h \gg \varepsilon$.

- The idea is to use suitable multiscale basis specific to the application in the DG method. Such basis should have explicit expressions if at all possible, in order to reduce computational cost
- Advantage: The DG method is quite flexible in its local approximation space (for each cell), as there is no continuity requirement at the cell boundary

- Advantage: Stability properties for DG methods usually only depend on the choice of the numerical fluxes, not the local approximation spaces
- Challenge: We must carefully analyze the errors associated with these discontinuities across element interfaces, to obtain convergence and (high order) error estimates

- Semiconductor devices: Schrödinger-Poisson system: Wang and Shu, JSC 09 (one-dimensional case). Two-dimensional work is ongoing research.

- Elliptic equations with oscillatory coefficients: Yuan and Shu, Int. J. Num. Meth Fluids 08; Wang, Guzmán and Shu, Int. J. Num. Anal. Mod. 11; Zhang, Wang, Guzmán and Shu, JSC to appear. Can handle the case of curvilinear unidirectional rough coefficients.

Energy conserving LDG methods for second order wave equations

We consider the second order wave equation

$$u_{tt} = \nabla \cdot (a^2(\boldsymbol{x}) \nabla u), \qquad \boldsymbol{x} \in \Omega, \quad t \in [0, T], \tag{15}$$

where $a(\boldsymbol{x}) > 0$ and can be discontinuous, subject to the initial conditions

$$u(\boldsymbol{x}, 0) = u_0(\boldsymbol{x}), \qquad u_t(\boldsymbol{x}, 0) = v_0(\boldsymbol{x}). \tag{16}$$

This equation can be converted to a standard first order hyperbolic system. DG scheme for such a system can be designed based on the standard upwind numerical flux. This DG scheme has the following features:

- It is energy dissipative: the total energy decays with time.
- It is optimal $(k+1)$-th order convergent with piecewise polynomials of degree k.

For nonlinear problems with discontinuous solutions, upwinding and its numerical dissipation are good to use. The resulting scheme is not only optimal convergent for smooth solutions but also stable for discontinuous solutions, with the capability of confining the errors in a small neighborhood of the discontinuity.

On the other hand, if we use a central numerical flux, then the resulting DG scheme has the following features:

- It is energy conserving: the total energy is constant in time.
- It is sub-optimal k-th order convergent with piecewise polynomials of degree k for some k.

Besides its sub-optimal convergence rate, the DG scheme with central flux is also very oscillatory when the solution becomes discontinuous.

However, if the exact solution is smooth and we would like to simulate the wave propagation over a long time period, then energy conserved numerical methods have advantages. We will show numerical evidence later. For first order hyperbolic systems, it is difficult to obtain DG schemes which are energy conservative and also optimal order convergent. Chung and Engquist (SINUM 06; SINUM 09) have proposed an optimal, energy conserving DG method for the first order wave equation using staggered grids.

On the other hand, we can directly approximate the second order wave equation by an LDG method. We prove that such LDG method is both energy conservative and optimal L^2 convergent (Xing, Chou and Shu, Inverse Problems and Imaging 13; Chou, Shu and Xing, JCP 14).

We numerically investigate the long time evolution of the L^2 error of the LDG method, in comparison with an IPDG method (Grote et al, SINUM 06) which conserves a specifically defined energy but not the usual energy. We consider again the wave equation

$$u_{tt} = u_{xx}, \qquad x \in [0,\ 2\pi]$$

with a periodic boundary condition $u(0,t) = u(2\pi, t)$ for all $t \geq 0$, and initial conditions $u(x,0) = e^{\sin x}$, $u_t(x,0) = e^{\sin x} \cos x$. This problem has the exact solution $u = e^{\sin (x-t)}$.

The LDG and IPDG methods are implemented with a uniform mesh with N cells, and the leap-frog time discretization, with $\Delta t = 0.6h^2$. In order to examine the potential shape difference resulted from long time integration, both methods are run until $T = 1000$, with finite element spaces P^2 and P^3, and $N = 40, 80$, respectively.

In Fig. 12, the time evolution of L^2 errors of both schemes are shown. The L^2 errors of both schemes grow in a linear fashion, but the slope for IPDG method is much larger than that for LDG method, which almost stays as constant and is close to zero. The errors are plotted in log scale for easy visualization. From the figure, one can see that for LDG method, the level of the errors are reduced by refining the mesh from $N = 40$ to $N = 80$, but the mesh refinement does not substantially reduce the errors of IPDG method due to the rapid growth.

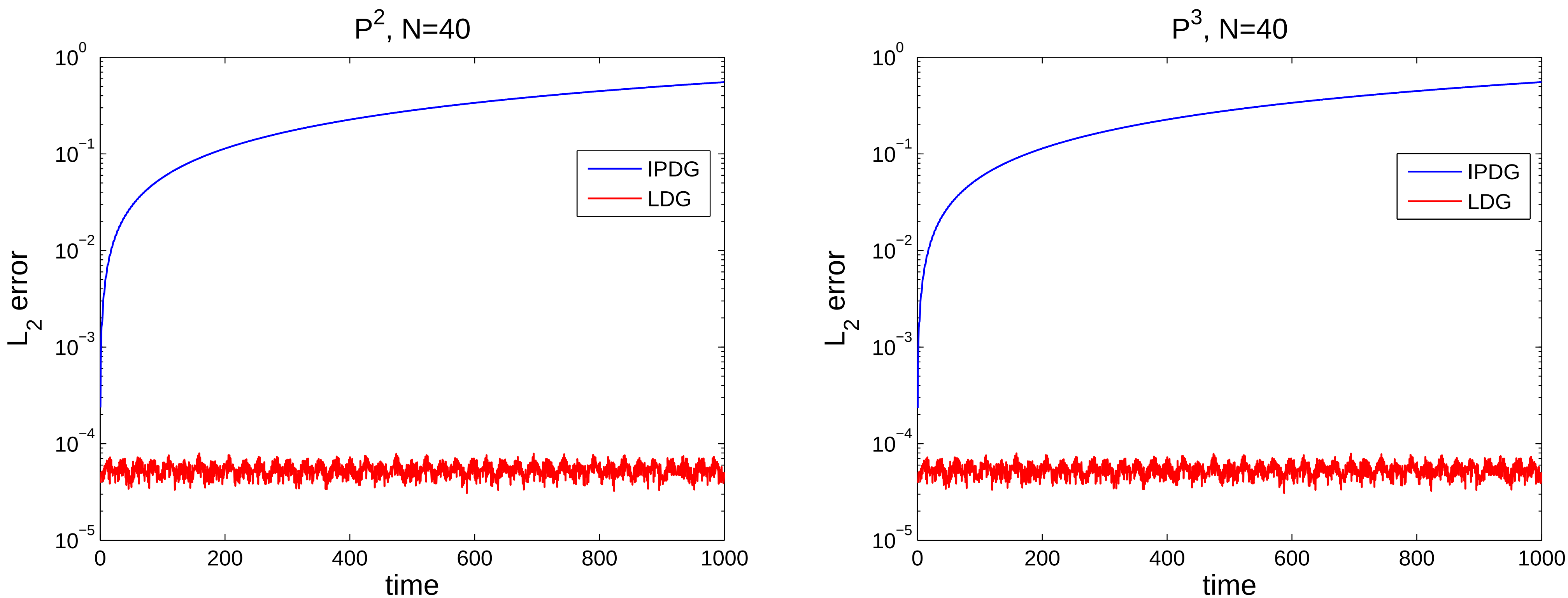

Figure 12: Time history until $T = 1000$ of the L^2 error of the numerical approximations obtained from the LDG and IPDG methods with $k = 2, 3$ and a uniform mesh with 40 cells. The L^2 error on y-axis are presented in log scale.

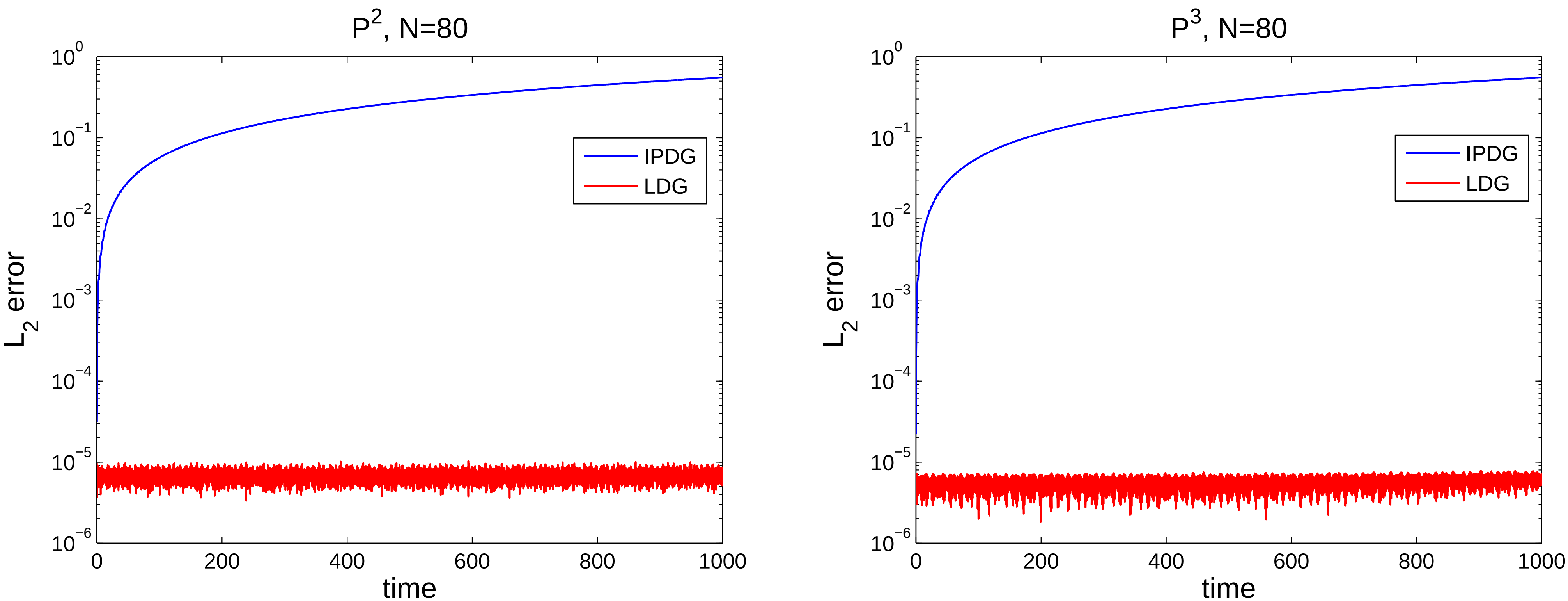

Figure 13: Time history until $T = 1000$ of the L^2 error of the numerical approximations obtained from the LDG and IPDG methods with $k = 2, 3$ and a uniform mesh with 80 cells. The L^2 error on y-axis are presented in log scale.

It can be observed from Fig. 12 that, up to $T = 1000$, the L^2 error of IPDG method is greater than 10^{-1}, and this large error can easily be visualized by directly comparing the solutions of both methods. Fig. 14 displays the exact solution (red), the solution of LDG method (green) and the solution of IPDG method (blue) at $T = 1000$, for spaces P^2 and P^3 with $N = 40$. It can be seen that solution of LDG method overlaps with the exact solution, while the solution of IPDG method preserves the shape but has a phase shift.

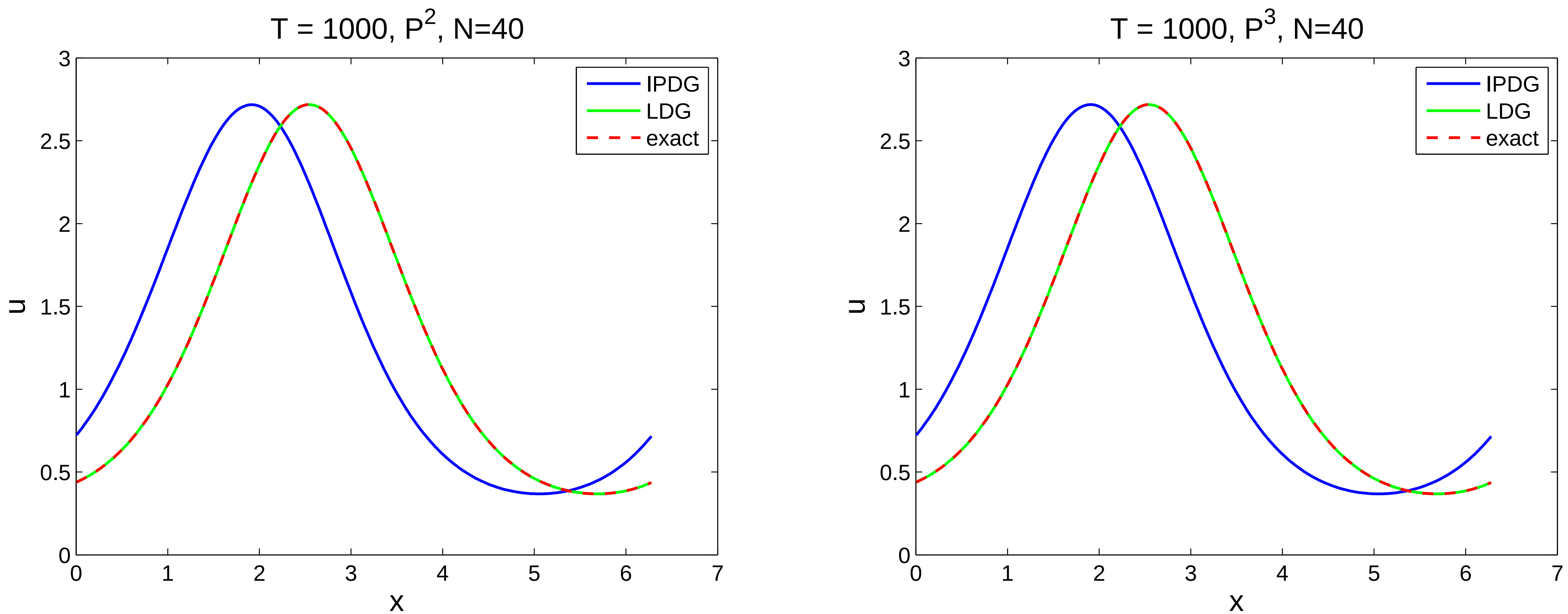

Figure 14: Numerical approximations of the wave equation using LDG and IPDG methods. Comparison is made at $T = 1000$ with $k = 2, 3$ and $N = 40$.

Higher order PDEs

LDG method for KdV equations

Now, the Korteweg-de Vries (KdV) equation:

$$u_t + (\alpha u + \beta u^2)_x + \sigma u_{xxx} = 0$$

More generally, in 1D:

$$u_t + f(u)_x + (r'(u) g(r(u)_x)_x)_x = 0$$

and in multi dimensions:

$$u_t + \sum_{i=1}^{d} f_i(u)_{x_i} + \sum_{i=1}^{d} \left(r_i'(u) \sum_{j=1}^{d} g_{ij}(r_i(u)_{x_i})_{x_j} \right)_{x_i} = 0$$

A “preview”: simple equation

$$u_t + u_{xxx} = 0$$

Again rewrite into a first order system

$$u_t + p_x = 0, \qquad p - q_x = 0, \qquad q - u_x = 0.$$

Then again *formally* use the DG method: find $u, p, q \in V_h$ such that, for all test functions $v, w, z \in V_h$,

$$\begin{aligned}
\int_{I_j} u_t v dx - \int_{I_j} p v_x dx + \hat{p}_{j+\frac{1}{2}} v^-_{j+\frac{1}{2}} - \hat{p}_{j-\frac{1}{2}} v^+_{j-\frac{1}{2}} &= 0, \\
\int_{I_j} p w dx + \int_{I_j} q w_x dx - \hat{q}_{j+\frac{1}{2}} w^-_{j+\frac{1}{2}} + \hat{q}_{j-\frac{1}{2}} w^+_{j-\frac{1}{2}} &= 0, \\
\int_{I_j} q z dx + \int_{I_j} u z_x dx - \hat{u}_{j+\frac{1}{2}} z^-_{j+\frac{1}{2}} + \hat{u}_{j-\frac{1}{2}} z^+_{j-\frac{1}{2}} &= 0.
\end{aligned}$$

Again, a key ingredient of the design of the LDG method is the choice of the numerical fluxes $\hat{u}$, $\hat{q}$ and $\hat{p}$ (now, upwinding principle partially available, after all, the solution with the initial condition $\sin(x)$ is $\sin(x+t)$, hence the wind blows from right to left).

The following choice of alternating + upwinding

$$\hat{p}_{j+\frac{1}{2}} = p^+_{j+\frac{1}{2}}, \qquad \hat{q}_{j+\frac{1}{2}} = q^+_{j+\frac{1}{2}}, \qquad \hat{u}_{j+\frac{1}{2}} = u^-_{j+\frac{1}{2}},$$

would guarantee stability. The choice is not unique:

$$\hat{p}_{j+\frac{1}{2}} = p^-_{j+\frac{1}{2}}, \qquad \hat{q}_{j+\frac{1}{2}} = q^+_{j+\frac{1}{2}}, \qquad \hat{u}_{j+\frac{1}{2}} = u^+_{j+\frac{1}{2}},$$

would also work.

Table 3: $u_t + u_{xxx} = 0$. $u(x,0) = \sin(x)$.

k		N=10	N=20		N=40		N=80
		error	error	order	error	order	error
0	L^2	2.2534E-01	1.2042E-01	0.91	6.2185E-02	0.95	3.1582E-02
	L^∞	4.3137E-01	2.1977E-01	0.97	1.1082E-01	0.98	5.5376E-02
1	L^2	1.7150E-02	4.2865E-03	2.00	1.0716E-03	2.00	2.6792E-04
	L^∞	5.8467E-02	1.5757E-02	1.89	4.0487E-03	1.96	1.0210E-03
2	L^2	8.5803E-04	1.0823E-04	2.98	1.3559E-05	2.99	1.6958E-06
	L^∞	4.0673E-03	5.1029E-04	2.99	6.4490E-05	2.98	8.0722E-06
3	L^2	3.3463E-05	2.1035E-06	3.99	1.3166E-07	3.99	8.2365E-09
	L^∞	1.8185E-04	1.1157E-05	3.97	7.2362E-07	3.99	4.5593E-08

Optimal in L^2 error estimates for not only u but also its derivatives can be proved. Xu and Shu, SINUM 2012.

The scheme can be designed for the general nonlinear case along the same lines.

For the general multi-dimensional nonlinear case

$$u_t + \sum_{i=1}^{d} f_i(u)_{x_i} + \sum_{i=1}^{d} \left(r_i'(u) \sum_{j=1}^{d} g_{ij}(r_i(u)_{x_i})_{x_j} \right)_{x_i} = 0$$

We can prove cell entropy inequality and L^2 stability. Yan and Shu, SINUM 02.

For the two dimensional KdV equation

$$u_t + f(u)_x + g(u)_y + u_{xxx} + u_{yyy} = 0,$$

and the Zakharov-Kuznetsov (ZK) equation

$$u_t + (3u^2)_x + u_{xxx} + u_{xyy} = 0,$$

We can prove error estimates of $O(h^{k+1/2})$ in L^2 for P^k elements in 1D and for Q^k elements in 2D, and of $O(h^k)$ for P^k elements in 2D. Yan and Shu, SINUM 02 (1D linear) and Xu and Shu, CMAME 07.

Numerical example: zero dispersion limit of conservation laws.

Solutions of the KdV equation with small dispersion coefficient

$$u_t + \left(\frac{u^2}{2}\right)_x + \epsilon u_{xxx} = 0. \tag{17}$$

with an initial condition

$$u(x,0) = 2 + 0.5\sin(2\pi x) \tag{18}$$

for $x \in [0,1]$ and periodic boundary conditions,

$\epsilon = 10^{-4}$, 10^{-5}, 10^{-6} and 10^{-7}.

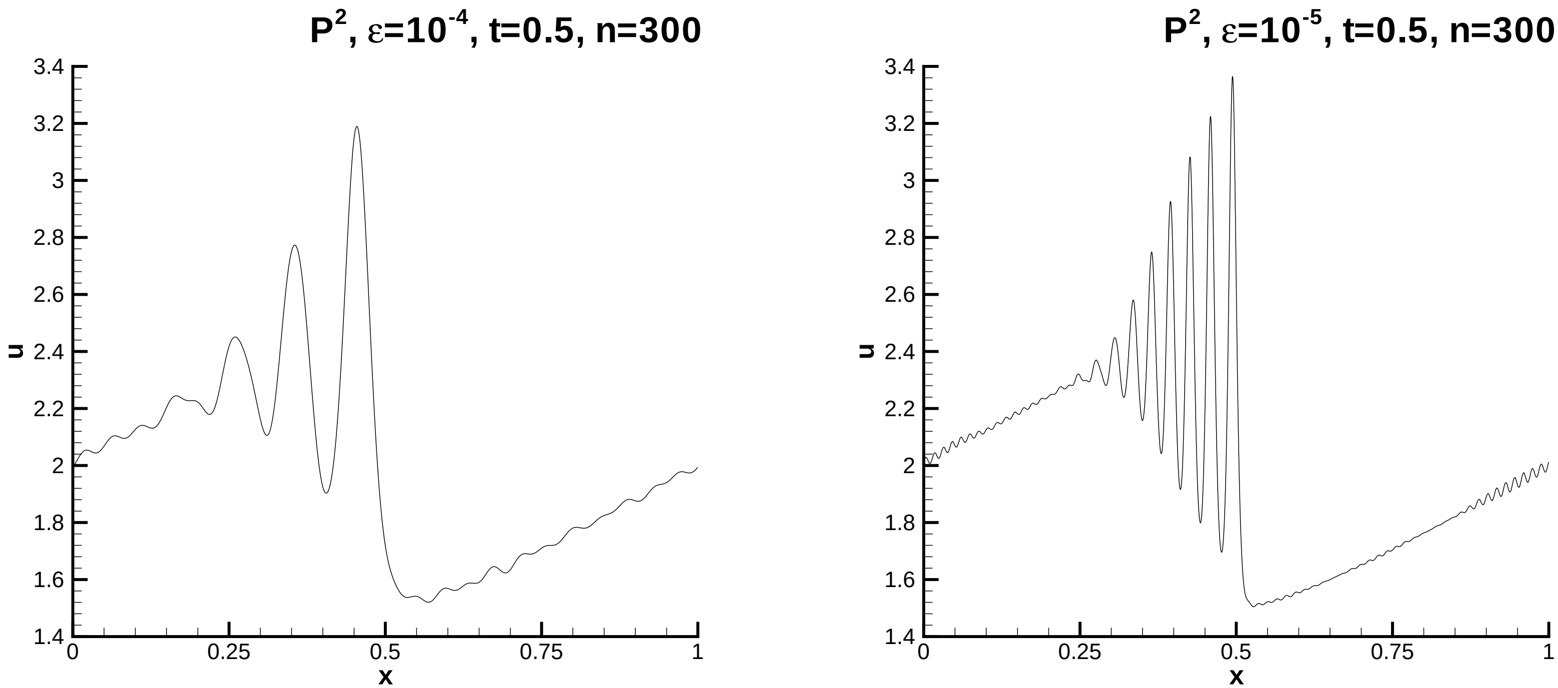

Figure 15: Zero dispersion limit of conservation laws. P^2 elements at $t = 0.5$. Left: $\epsilon = 10^{-4}$ with 300 cells; right: $\epsilon = 10^{-5}$ with 300 cells.

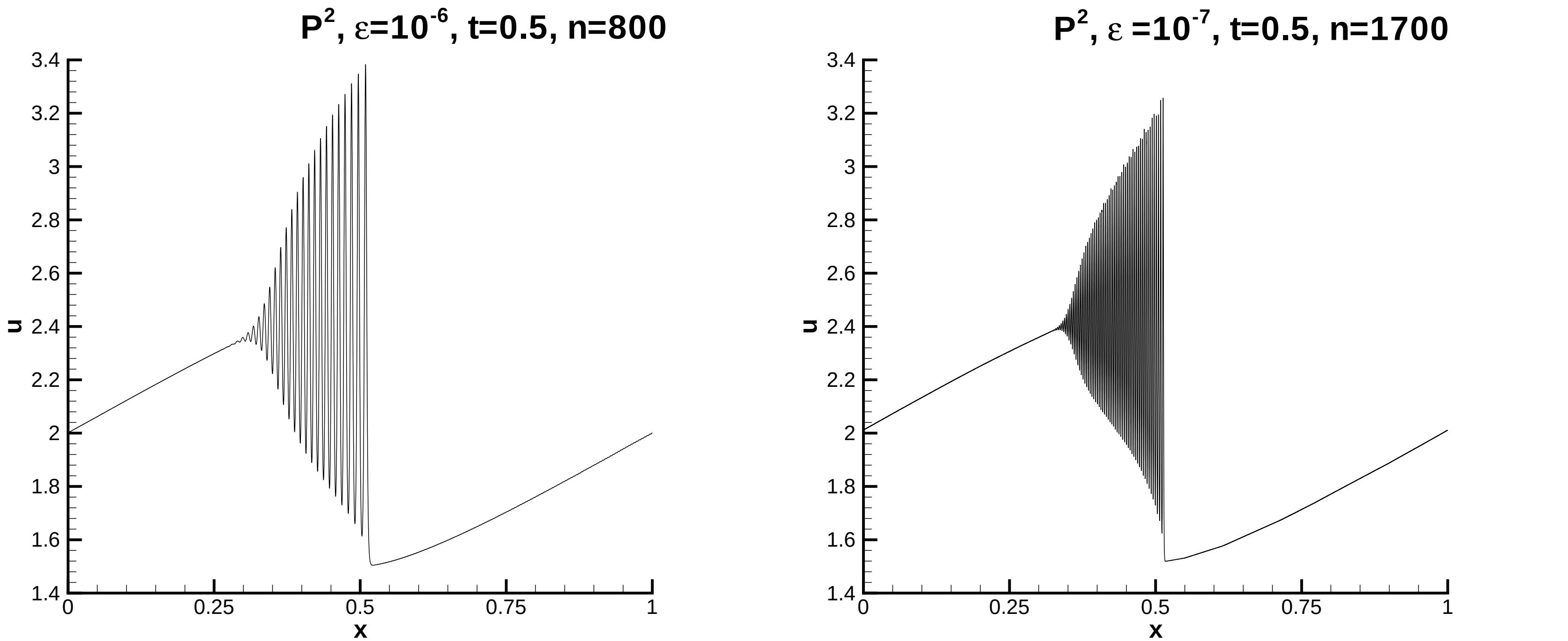

Figure 16: Zero dispersion limit of conservation laws. P^2 elements at $t = 0.5$. Left: $\epsilon = 10^{-6}$ with 800 cells; right: $\epsilon = 10^{-7}$ with 1700 cells.

LDG methods for other diffusive equations

- The bi-harmonic type equation

$$u_t + \sum_{i=1}^{d} f_i(u)_{x_i} + \sum_{i=1}^{d} (a_i(u_{x_i}) u_{x_i x_i})_{x_i x_i} = 0 \qquad (19)$$

We can prove a cell entropy inequality and L^2 stability Yan and Shu, JSC 02 for the general nonlinear problem and an optimal L^2 error estimates Dong and Shu, SINUM 09 for the linear biharmonic and linearized Cahn-Hilliard equations.

Both the schemes and the analysis can be generalized to higher even order diffusive PDEs, e.g. the error estimate in Dong and Shu, SINUM 09 is given also for higher even order linear diffusive PDEs.

- The Kuramoto-Sivashinsky type equations

$$u_t + f(u)_x - (a(u)u_x)_x + (r'(u)g(r(u)_x)_x)_x + (s(u_x)u_{xx})_{xx} = 0, \tag{20}$$

We prove a cell entropy inequality and L^2 stability in Xu and Shu, CMAME 06.

- Device simulation models in semi-conductor device simulations: drift-diffusion, hydrodynamic, energy transport, high field, kinetic and Boltzmann-Poisson models, formulations of DG-LDG schemes and error estimates. Liu and Shu, JCE 04; ANM 07; Sci in China 10; Cheng, Gamba, Majorana and Shu, JCE 08; CMAME 09.

- Cahn-Hilliard equation

$$u_t = \nabla \cdot \Big(b(u)\nabla\big(-\gamma\Delta u + \Psi'(u)\big)\Big), \qquad (21)$$

and the Cahn-Hilliard system

$$\mathbf{u}_t = \nabla \cdot (\mathbf{B}(\mathbf{u})\nabla\omega), \qquad \omega = -\gamma\Delta\mathbf{u} + D\Psi(\mathbf{u}), \qquad (22)$$

where $\{D\Psi(\mathbf{u})\}_l = \frac{\partial\Psi(\mathbf{u})}{\partial u_l}$ and γ is a positive constant. We design LDG methods and prove the energy stability for the general nonlinear case in Xia, Xu and Shu, JCP 07; CiCP 09.

- The surface diffusion equation

$$u_t + \nabla \cdot \left(Q \left(\boldsymbol{I} - \frac{\nabla u \otimes \nabla u}{Q^2} \right) \nabla H \right) = 0 \tag{23}$$

where

$$Q = \sqrt{1 + |\nabla u|^2}, \qquad H = \nabla \cdot \left(\frac{\nabla u}{Q} \right) \tag{24}$$

and the Willmore flow

$$u_t + Q\nabla \cdot \left(\frac{1}{Q} \left(\boldsymbol{I} - \frac{\nabla u \otimes \nabla u}{Q^2} \right) \nabla (QH) \right) - \frac{1}{2} Q \nabla \cdot \left(\frac{H^2}{Q} \nabla u \right) = 0 \tag{25}$$

We develop LDG methods and prove their energy stability in Xu and Shu, JSC 09.

LDG methods for other dispersive wave equations

- The partial differential equations with five derivatives

$$U_t + \sum_{i=1}^{d} f_i(U)_{x_i} + \sum_{i=1}^{d} g_i(U_{x_ix_i})_{x_ix_ix_i} = 0 \qquad (26)$$

We can prove a cell entropy inequality and L^2 stability, Yan and Shu, JSC 02.

- The $K(m,n)$ equation

$$u_t + (u^m)_x + (u^n)_{xxx} = 0,$$

with *compactons* solutions. We obtain a L^{n+1} stable LDG scheme for the $K(n,n)$ equation with odd n, and a linearly stable LDG scheme for other cases, Levy, Shu and Yan, JCP 04.

- The KdV-Burgers type (KdVB) equations

$$u_t + f(u)_x - (a(u)u_x)_x + (r'(u)g(r(u)_x)_x)_x = 0 \tag{27}$$

We prove a cell entropy inequality and L^2 stability, and obtain L^2 error estimate of $O(h^{k+1/2})$ for the linearized version in Xu and Shu, JCM 04.

- The fifth-order KdV type equations

$$u_t+f(u)_x+(r'(u)g(r(u)_x)_x)_x+(s'(u)h(s(u)_{xx})_{xx})_x=0 \quad (28)$$

  We prove a cell entropy inequality and L^2 stability in Xu and Shu, JCM 04.

- The fifth-order fully nonlinear $K(n,n,n)$ equations

$$u_t+(u^n)_x+(u^n)_{xxx}+(u^n)_{xxxxx}=0 \quad (29)$$

  We prove L^{n+1} stability for odd n in Xu and Shu, JCM 04.

- The generalized nonlinear Schrödinger (NLS) equation

$$i\,u_t + \Delta u + f(|u|^2)u = 0, \tag{30}$$

and the coupled nonlinear Schrödinger equation

$$\begin{cases} i\,u_t + i\,\alpha u_x + u_{xx} + \beta\,u + \kappa v + f(|u|^2, |v|^2)u = 0 \\ i\,v_t - i\,\alpha v_x + v_{xx} - \beta\,u + \kappa v + g(|u|^2, |v|^2)v = 0 \end{cases} \tag{31}$$

We prove a cell entropy inequality and L^2 stability, and obtain L^2 error estimate of $O(h^{k+1/2})$ for the linearized version in Xu and Shu, JCP 05.

- The Ito-type coupled KdV equations

$$\begin{aligned} u_t + \alpha u u_x + \beta v v_x + \gamma u_{xxx} &= 0, \\ v_t + \beta (uv)_x &= 0, \end{aligned}$$

We prove a cell entropy inequality and L^2 stability in Xu and Shu, CMAME 06.

- The Kadomtsev-Petviashvili (KP) equation

$$(u_t + 6uu_x + u_{xxx})_x + 3\sigma^2 u_{yy} = 0, \tag{32}$$

where $\sigma^2 = -1$ (KP-I) or $\sigma^2 = 1$ (KP-II). We design an LDG method and prove the L^2 stability in Xu and Shu, Physica D 05.

- The Zakharov-Kuznetsov (ZK) equation

$$u_t + (3u^2)_x + u_{xxx} + u_{xyy} = 0. \tag{33}$$

We prove the L^2 stability in Xu and Shu, Physica D 05.

- The Camassa-Holm (CH) equation

$$u_t - u_{xxt} + 2\kappa u_x + 3uu_x = 2u_x u_{xx} + uu_{xxx}, \tag{34}$$

where κ is a constant. We prove the L^2 stability and provide L^2 error estimates for the LDG method in Xu and Shu, SINUM 08.

- The Hunter-Saxton (HS) equation

$$u_{xxt} + 2u_x u_{xx} + u u_{xxx} = 0, \tag{35}$$

its regularization with viscosity

$$u_{xxt} + 2u_x u_{xx} + u u_{xxx} - \varepsilon_1 u_{xxxx} = 0, \tag{36}$$

and its regularization with dispersion

$$u_{xxt} + 2u_x u_{xx} + u u_{xxx} - \varepsilon_2 u_{xxxxx} = 0, \tag{37}$$

where $\varepsilon_1 \geq 0$ and ε_2 are small constants. We design LDG methods and prove the energy stability in Xu and Shu, SISC 08; JCM 10.

- The generalized Zakharov system:

$$
\begin{aligned}
iE_t + \Delta E - Nf(|E|^2)E + g(|E|^2)E = 0, \\
\epsilon^2 N_{tt} - \Delta(N + F(|E|^2)) = 0,
\end{aligned}
$$

which is originally introduced to describe the Langmuir turbulence in a plasma. We prove two energy conservations for the LDG method in Xia, Xu and Shu, JCP 10.

- The Degasperis-Procesi (DP) equation

$$u_t - u_{txx} + 4f(u)_x = f(u)_{xxx}, \tag{38}$$

where $f(u) = \frac{1}{2}u^2$. The solution may be discontinuous regardless of smoothness of the initial conditions. We develop LDG methods and prove L^2 stability for the general polynomial spaces and total variation stability for P^0 elements Xu and Shu, CiCP 11.

The End

THANK YOU!